Development of a 3D Navigated Surgical Cutting Guide

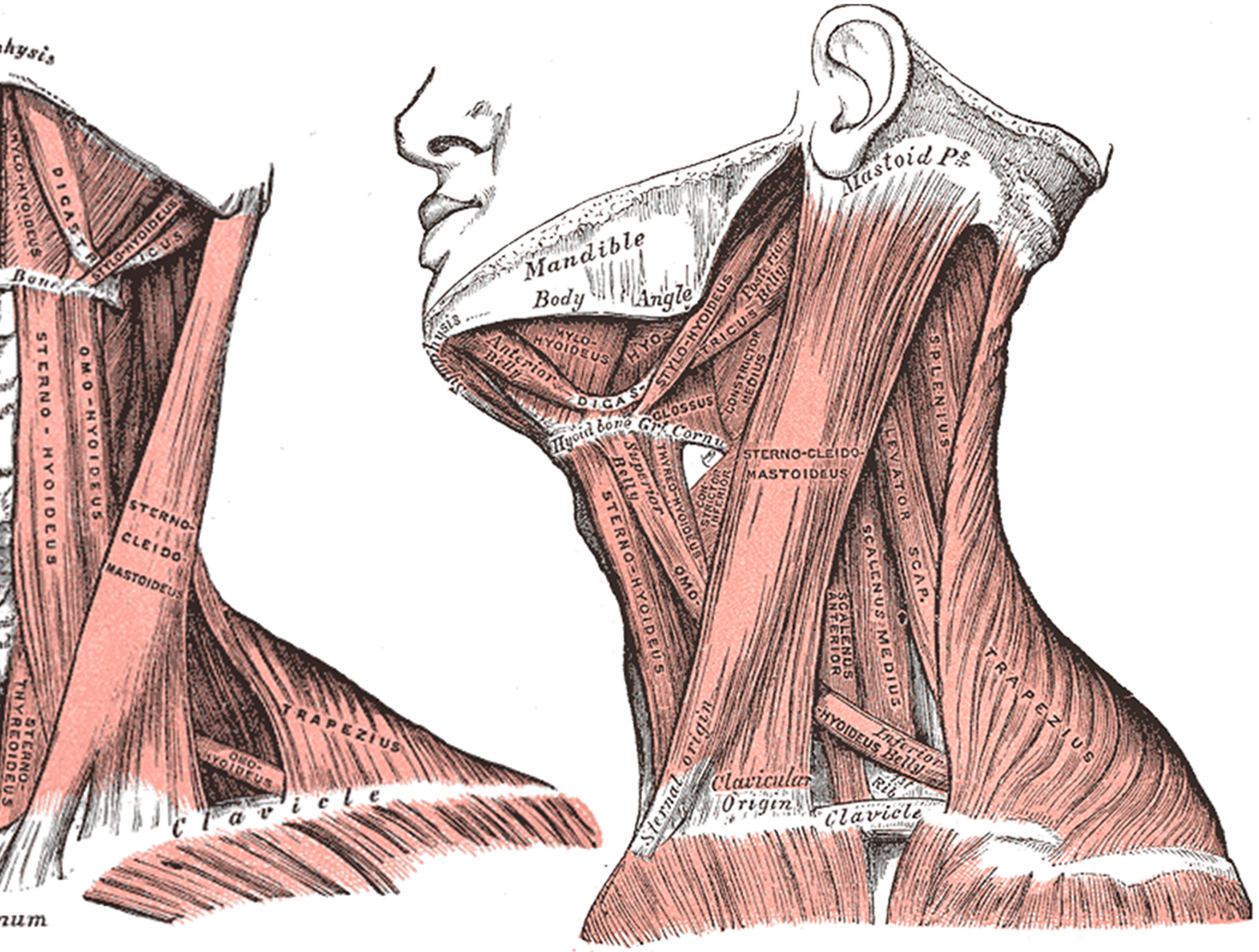

T.P. ter Braak

Technical Medicine - Master Thesis

University of Twente

06-09-2019

ANTONI VAN LEEUWENHOEK
NEDERLANDS KANKER INSTITUUT

UNIVERSITY OF TWENTE.

Master Thesis Technical Medicine
Medical Imaging & Intervention

Development of a 3D Navigated Surgical Cutting Guide

Timon ter Braak
s1366637

Graduation Committee

Chairman	dr. ir. F. van der Heijden
Medical supervisor	dr. M.B. Karakullukcu
Technical supervisor	dr. ir. F. van der Heijden
Process supervisor	drs. B.J.C.C. Hessink-Sweep
Additional member	dr. M.J.A. van Alphen
External member	dr. E. Groot Jebbink

Friday, 6 September 2019

Summary

Background: The gold standard treatment for tumour invading the mandibular bone, is surgical resection of the bone and reconstruction with autogenous bone flaps. Currently, the mandibular osteotomies are performed using patient-specific three-dimensional (3D) printed cutting guides. These guides allow the location and orientation of the planned osteotomies to be replicated accurately during surgery, however they still have shortcomings. These guides do not allow for alterations of the preoperative planning and have a lengthy time interval between planning and surgery due to design and production. Both the inability to allow alterations and the lengthy time interval negatively influence the surgical result. In this study, a navigated cutting guide is proposed along with an improved registration method for mandibular osteotomies.

Registration: The current registration method using intraoperative cone beam computed tomography takes surgery time and has a low resolution, limiting the registration accuracy. Five different registration methods utilising splints, screws or combinations are evaluated. A dental and edentate phantom model of a mandible were created and scanned according to the regular preoperative computed tomography protocol, together with the splint/screws for the registration. Surgical navigation was performed with the NDI Aurora planar field generator. A point-match procedure was performed for the registration, thereafter the target registration error was determined along the surface on a total of 45 points for the dental and 35 points for the edentate model. The dental splint with incorporated registration fiducials performed best, with a root mean square error of 0.89 mm, which is a clear improvement on the 2.1 mm of the current registration method.

Navigated cutting guide: A navigated cutting guide has been developed, consisting of three elements which allow for fixation to the mandible while still enabling adjustments in position and orientation. A total of twenty osteotomies have been performed on ten plaster mandibles, and evaluated on accuracy in position and orientation. The median deviation in position was 1.0 mm and in orientation 1.6° for the yaw and 1.1° for the roll. The results were compared with preliminary clinical data of the 3D printed cutting guides and a navigated saw study found in literature. There was no significant difference in the deviation of the position ($p = 0.640$), but there were significant differences in both the yaw and the roll. In the yaw, there were statistically significant differences between the navigated cutting guide with the navigated saw ($p < 0.001$) and with the 3D printed cutting guide ($p = 0.035$). In the roll, there were statistically significant differences between the navigated cutting guide with the navigated saw ($p = 0.018$) and with the 3D printed cutting guide ($p = 0.043$). In conclusion, despite the initial stages of the research, encouraging results were obtained.

Contents

Introduction

1

1.1 The mandible

> *The word "mandible" derives from the Latin word mandibula, "jawbone" (literally "one used for chewing"), from mandere "to chew" and -bula (instrumental suffix).*

1.1.1 Anatomy

The mandible, or lower jaw, forms the caudal part of the bony base of the oral cavity (Fig 1.1). It is the only movable bone of the skull (discounting the ossicles of the middle ear). The body of the mandible is curved, and is important in providing aesthetics of the face. The main function of the mandible is mastication, but also plays a role in swallowing, speaking and breathing [1]. Four different muscles connect to the mandible to facilitate its movement. These muscles are the masseter, the temporalis, the pterygoid internus, and the pterygoid externus [2]. Each of these muscles occur in pairs, with one of each muscle appearing on either side of the skull. The muscles work in combination to pivot the mandible up and down and to allow movement of the jaw from side to side. The other muscles connecting to the maxilla, hyoid bone or tongue perform various functions to facilitate chewing, swallowing, speaking and breathing.

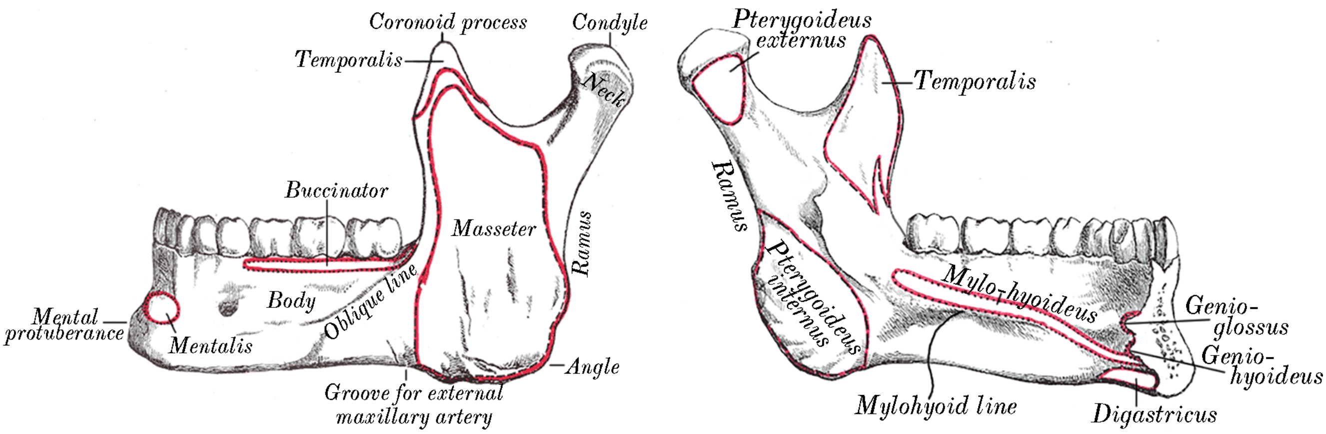

(a) lateral surface, side view

(b) medial surface, side view

Fig. 1.1: Anatomy of the mandible with muscular attachments indicated in red [3].

1.2 Mandibular cancer

1.2.1 Epidemiology

Primary bone tumours of the mandible are rare [4]. According to different studies the incidence of mandibular bone involvement in oral cancer ranges from 12% to 56% [5]. Over the past decades the incidence of oral cavity cancer (OCC) has seen a steady increase. In the Netherlands, 940 patients were diagnosed with OCC in the year 2017, which equals to 5.5 cases per 100.000 residents [6]. Worldwide, over 350.000 new cases of OCC are diagnosed each year, with twice as many male as female incidences [7]. The risk of developing OCC increases with age, with the majority of cases occurring at or after the fifth decade of life [8]. Risk factors include: smoking, alcohol consumption and human papillomavirus (HPV) infections with smoking and alcohol use having synergistic and cumulative effects [8, 9].

1.2.2 Diagnosis

The most common symptom of OCC is pain, representing 30-40% of patient complaints [10]. This pain usually presents itself after the primary lesion has reached a considerable size, which leads to a late diagnosis [11]. Other common symptoms include trouble with speech or swallowing, ear pain, bleeding, loosening of teeth, ill-fitting dentures or a reduced opening of the jaw [10–13]. The first step of the diagnosis starts with a physical examination. If visual inspection and/or palpation has suspicious findings, the patient undergoes additional imaging. This can be in the form of computed tomography (CT), magnetic resonance imaging (MRI), single photon emission computed tomographic (SPECT), and/or ultrasound (US) scans. A biopsy can also be performed to establish the presence and type of a tumour.

1.2.3 Treatment

Surgery and chemotherapy are the two most important treatment options for OCC. Surgery is the preferred first treatment, as it leaves more options in case of tumour recurrence. It is well recognised and documented that tumours invading the mandibular bone are unlikely to be cured by radiation therapy alone and require partial or hemimandibulectomy to provide adequate surgical margins [5]. The goal of the surgery is a radical excision of the tumour, while other vital structures are spared as much as possible. Larger resections would have implications for the patients speech, swallowing and mastication [14].

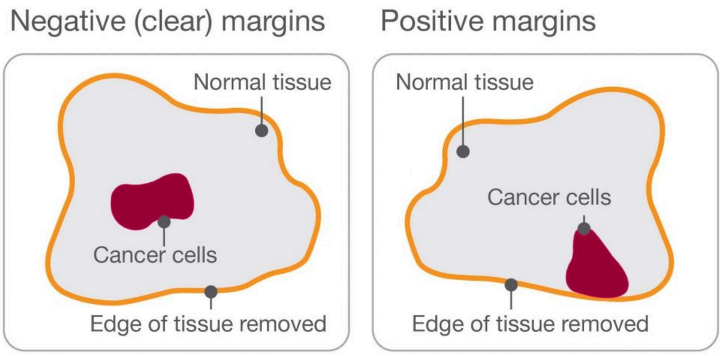

Fig. 1.2: Visual explanation of negative (clear) and positive margins. Negative (clear) margins mean no cancer cells were seen at the outer edge of the tissue removed. Positive margins mean the cancer cells are very close to or reach the edge of the tissue [15].

1.2.4 Surgical margins

During the surgery, the surgeon aims to resect a 10 mm rim of clinically normal tissue around a tumour in order to give a 'margin' of normal tissue (Fig. 1.2) [12, 14]. After the surgery, tissue shrinkage will occur during fixation and pathological processing, which means that the 'pathological' margin is less than the true 'surgical' margin [14]. A histological resection margin of 5 mm is generally accepted [16, 17]. For mandibular invasion, surgery should be performed with 1 cm bony margins around the tumour as determined by a radiologist in the imaging data [12]. Positive margins impart a poor prognosis on the patient, both in terms of local recurrence and overall survival [14] as a recurrence arising from failures to control the local disease is the usual cause of death [5].

1.2.5 Reconstruction

After surgery where a (partial) mandibulectomy has been performed, the defect needs to be reconstructed to restore both form and function. The goals of mandibular reconstruction are to re-establish the facial contours and to restore the patient's ability to eat in public, be intelligible to both trained and untrained listeners, and to maintain a free airway that allows the patient to perform all activities [19]. There is a variety of reconstruction methods using alloplastic or autogenous material [20, 21]. The plate-only method uses a titanium plate to bridge the segmental defect. Plate fracture and exposure tend to be the most frequently encountered complications and the risk increases the longer the plate is in place. Therefore, this mode of reconstruction may not be the best option for a young patient with a long life expectancy [21]. Most often this reconstruction plate is combined with a vascularised bone flap, from the scapula, radial, iliac crest or the fibula [20, 21].

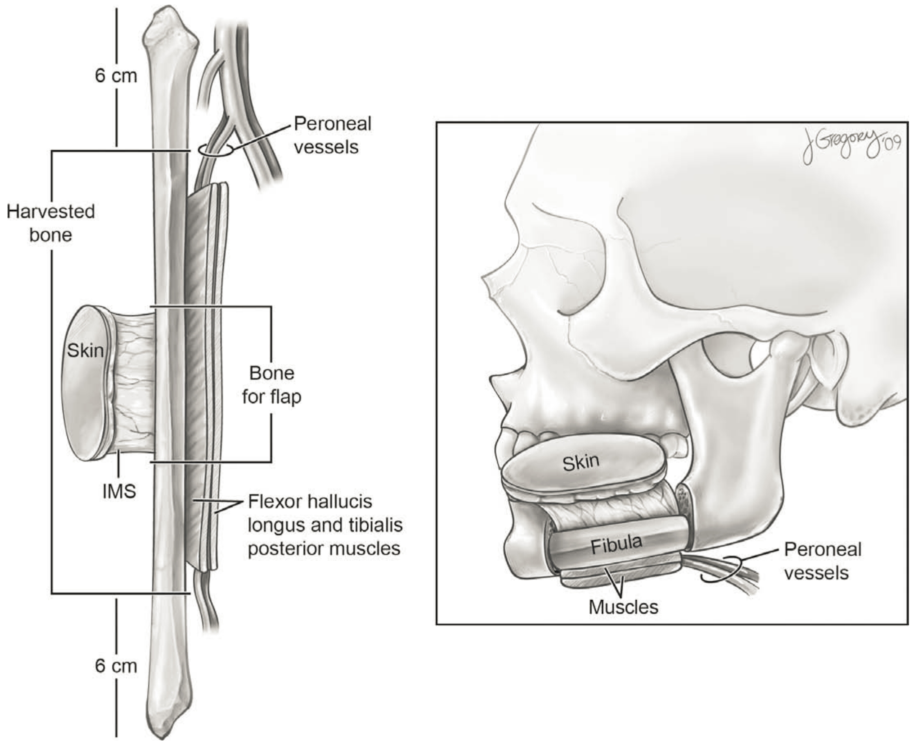

Fig. 1.3: Anatomy of fibular free flap and example of segmental defect with fibular flap inset [18]. IMS, intermuscular septum.

Where the fibular osteocutaneous free flap (Fig. 1.3) is the golden standard donor site for mandibular reconstruction [19, 22–25]. The known advantages are an abundant supply of bicortical bone that is available for reconstruction of defects across the midline, eligibility for the subsequent insertion of dental implants, the opportunity for simultaneous dissection of the fibula while operating at the head, and little morbidity of the donor site [19].

1.3 Clinical problem

Currently, prior to the surgery, a pre-operative planning is made in a virtual environment. The goal of the planning is to obtain sufficient resection margins and to create an outline for the reconstruction. The boundaries of the resection in the mandible are placed accurately in safe tissues. From the planned defect, it can be determined how many fibular pieces with length and angle specifications are required to fill the defect. If necessary, small alterations can be made to the resection planes to benefit the reconstruction. Using this planning, surgical cutting guides (Fig. 1.4) can be developed, which allow the location and orientation of the planned osteotomies to be replicated accurately during surgery [26, 27]. Consequently, operating time and cost is reduced as there is no need to approximately and repeatedly model the fibular segment to the native mandible (as is conventional in procedures without the surgical guides) [26–29].

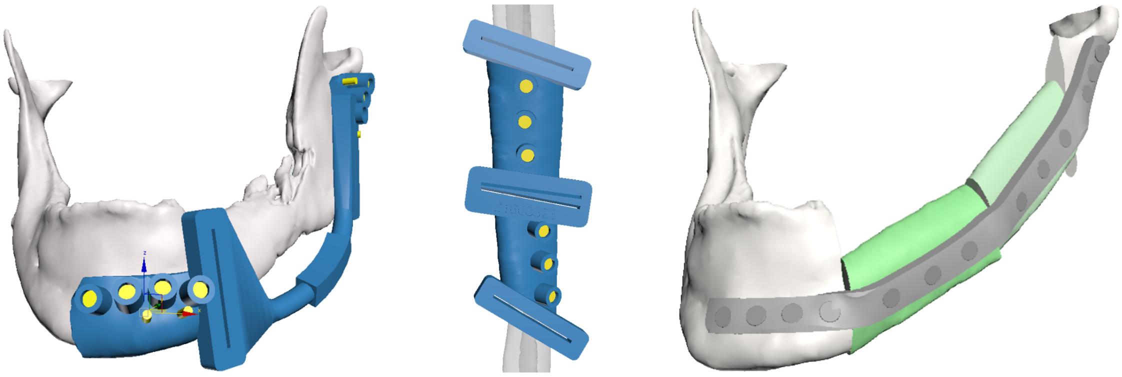

(a) Mandibular cutting guide **(b)** Fibular cutting guide **(c)** Planned reconstruction result

Fig. 1.4: Example of a surgical cutting guide used in surgery at the Netherlands Cancer Institute, with the corresponding planned reconstruction. The guides are fixated with screws through the small holes indicated in yellow. The bone is cut by placing a saw through the long slits.

Although this virtual surgical planning has made the outcome more predictable and accurate compared to the free-hand approach, several shortcomings and problems still occur using this approach. The time interval between the planning CT and the surgery should not exceed two weeks [26], but nonetheless can take as long as four weeks or more. Even a two-week delay may result in serious limitations for patients with rapidly growing tumors or acute trauma [30]. Positioning of the three-dimensional (3D) printed cutting guide can be inaccurate due to remaining soft tissue between the mandible and the cutting guide, resulting in aberrant cutting planes. If a non-perfect fit is noticed or an unexpected intraoperative finding occurs, the non-flexibility of the cutting guides does not allow for alterations of the original planning [26]. On top of that, the printed material lacks robustness, making it possible for the surgical saw to cut through the 3D printed cutting guide resulting in a non-straight cut. The dependence on an external medically certified 3D printing company and the frequently complicated and time-consuming logistics and communication between engineer, surgeon, operating department/nurses and sterilisation department result in overall costly 3D printed cutting guides [31]. A novel approach that overcomes the disadvantages of 3D printed cutting guides is therefore required. The aim of this study is to develop a surgical navigation procedure for mandibular surgery and evaluate its feasibility and accuracy, to provide guidance during and decrease the delay before surgery.

1.4 Thesis outline

In this thesis, a navigated cutting guide is proposed as an alternative for 3D printed cutting guides. First, in chapter 2 an introduction into surgical navigation is provided with current tracking methods and applications, following into the technical medical problems and objectives in section 2.4. In chapter 3, a solution for the first problem; registration in surgical navigation for mandibular surgery, is given. The navigated cutting guide is introduced and evaluated in chapter 4, following in the overall conclusion in chapter 5 and ending in the future perspectives in chapter 6.

2 Surgical navigation

> *The word "navigation" derives from Latin "navigatio(n-)" (denoting travel on water), from the verb "navigare". Navigation is the process or activity of accurately ascertaining one's position and planning and following a route.*

Currently, the surgical guides are created patient specific, making them accurate and easy to use, but very inflexible in their use. To overcome this problem, a universal cutting guide in combination with surgical navigation is proposed. Surgical navigation can provide the surgeon with real-time visual feedback about his current instrument position in relation to the patients anatomy and tumour [32]. The position and orientation of the different cutting planes can be derived from this feedback, which can consequently be translated to cutting planes in the fibula. In this chapter, an introduction into surgical navigation is provided following into the technical medical problems and objectives.

2.1 Principle of surgical navigation technology

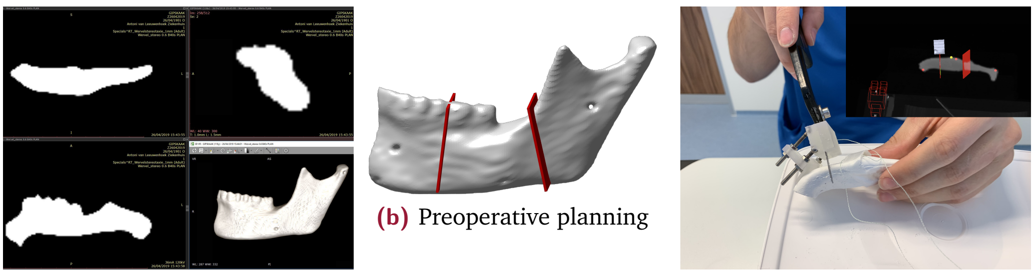

(a) Preoperative imaging **(b)** Preoperative planning **(c)** intraoperative execution

Fig. 2.1: Visual representations of the three principles of surgical navigation; preoperative imaging, preoperative planning, intraoperative execution of an osteotomy performed on a plaster mandible model.

Surgical navigation can be divided in three steps: preoperative imaging, preoperative planning and intraoperative execution [33], seen in figure 2.1. In the first step, a better understanding is required of the anatomy of the patient and the location of the tumour. Therefore, the patient requires one or more preoperative scans. In the second step, the location of the tumour is evaluated and a 3D model is created of the patients anatomy including the tumour. Resection of the tumour can be planed in this 3D model, taking the surgical margins into account [34]. In the third and final step, a registration is required to match the coordinate system of the 3D model and the preoperative imaging to that of the current patient position in the operating room (OR) [32, 35, 36]. Different methods exist, such as point-match and surface-match registration which both use a tracked pointer [36]. Point-match uses artificial or anatomical landmarks, indicated on both the patient and the 3D model. With a surface-match, the tool is dragged over the patients anatomy to indicate a surface and match it with the model. After registration the real-time position of a tracked surgical tool can be shown in the 3D model of the patient on the OR screens.

2.2 Electromagnetic vs. optical tracking

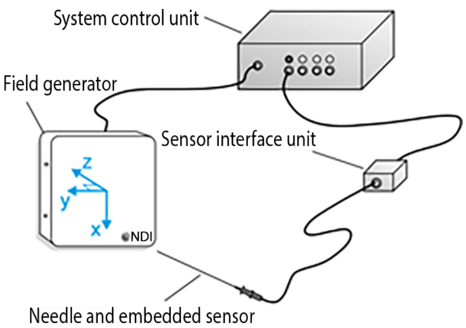

(a) Electromagnetic navigation [37]

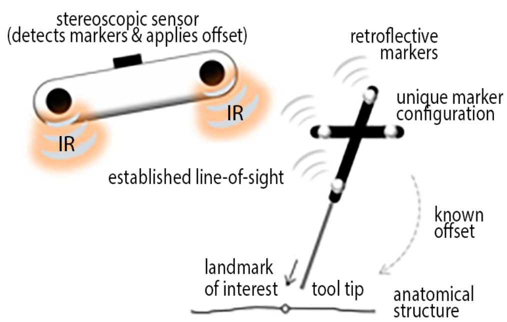

(b) Optical navigation [38]

Fig. 2.2: Schematic diagrams of electromagnetic and optical tracking technology

Two main tracking methods exist: Electromagnetic (EM) and optical (Fig. 2.2). The EM tracking system generates its own electromagnetic field, which induces currents in the sensors based on magnetic induction [35]. These currents provide the system with information about the position and orientation of the sensors connected to the surgical tools and the patient. A disadvantage of EM tracking is that the accuracy is susceptible to nearby metal objects, as they can cause magnetic field distortions [32, 35]. Optical tracking uses an infrared camera system and infrared reflecting spheres attached to surgical tools and the patient. The spheres need to be seen in multiple cameras to calculate the distance from the cameras and the orientation of the tools and patient in space. The accuracy of optical tracking is higher than that of EM tracking, but it requires a constant line-of-sight. The required direct line-of-sight in optical tracking, limits the surgeons flexibility and is difficult to guarantee in practice, especially in small working areas like head and neck surgery [39]. Therefore, EM tracking has been chosen for this study.

2.3 Current clinical applications of EM tracking in head and neck surgery

Infrared-based optical navigation systems are the current standard for intraoperative navigation in head and neck surgery [40]. However, developments in hardware and software have helped stabilise and improve the accuracy and stability of EM tracking increasing its popularity [41]. In literature, most reports of EM tracking in the head and neck area are in phantom skull studies or single case reports. These promising studies show similar accuracy as that of optical tracking [39, 41–43]. Navigation during mandibular surgery is reported, but these studies focus on segment positioning in orthognathic surgery [44, 45] and marking osteotomy positions using a navigated pen [42]. Recently, two research groups have been working on a navigated saw for performing virtually-planned mandibular osteotomies [46, 47]. However, surgical navigation of a cutting guide for mandibular osteotomies has not yet been performed, as far as known.

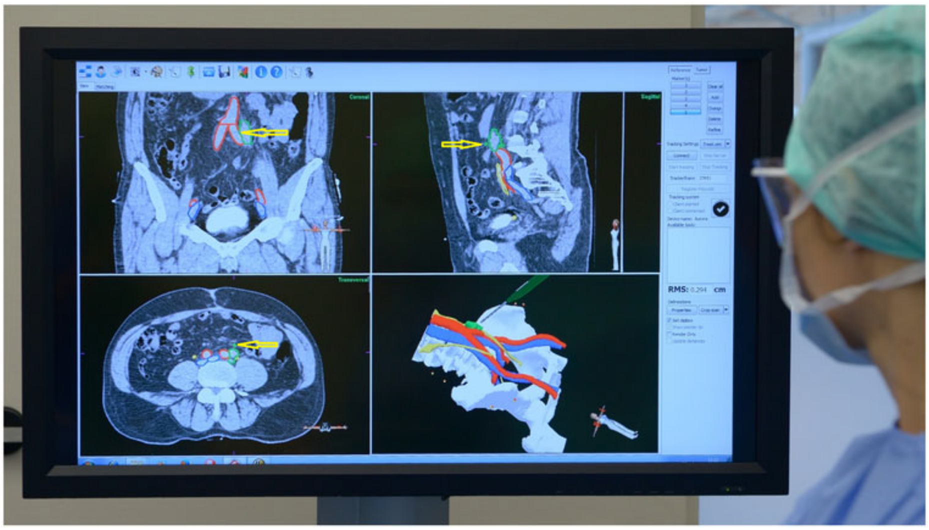

Fig. 2.3: Picture of the surgical navigation user interface "SurgNav" during laparoscopic surgery [48].

The Netherlands Cancer Institute (NKI) utilises an in-house developed navigation software, *SurgNav* (Fig 2.3) [48], in combination with an EM tracking system, NDI Aurora (Northern Digital Inc., Waterloo, Canada), which is currently applied in liver, lymph node and rectal surgery. The system allows for real-time tracking of sensor locations and orientations inside a 3D measuring volume. The software accommodates a four-display mode (axial, sagittal, frontal, and 3D) where the position and orientation of the tools relative to the imaging data are visualised. In a hybrid OR an intraoperative CT scan is made of the patient, which is first registered to the preoperative imaging using bone-bone registration and then to the navigation system using a point-match with anatomical or intraoperative placed markers.

2.4 Technical medicine problems and objectives

In a previous graduation internship, a start was made with the development of a surgical navigation method for OCC using EM tracking [49]. In this study, the current 3D printed cutting guides were attached to the mandible using screws, and subsequently an intraoperative CT scan was made. These screws were then used to register the mandible in the EM field, as this has an increased accuracy as opposed to anatomical landmarks [49].

This method is difficult to reproduced in case of a 3D navigated cutting guide, as the placement of this guide requires the registration to be performed beforehand. Additionally, the intraoperative CT scan has a lower resolution and takes about half to a full hour of OR time which is expensive and not beneficial to the overall procedure. Anatomical landmarks could be used for the registration which would eliminate the intraoperative CT scan. However, anatomical landmarks have been proven to be less accurate than man-made markers. Therefore, a new registration method is required which utilises man-made markers without using the intraoperative CT scan, resulting in the first objective:

- Develop and evaluate an intraoperative registration method without intraoperative imaging, to translate the virtual surgical planning to the OR.

Surgical navigation provides visual feedback of the instruments position and orientation in relation to the patients anatomy. Thought should be given as to how the planning is presented, to support the positioning of the universal guide. The surgical navigated positioning of the navigated cutting guide, should have the same or higher precision as the current 3D printed cutting guides to ensure sufficient surgical margins. For the reconstruction, the length of the defect and the angles of the cutting planes need to be converted to cutting planes in the fibula. Another graduating technical medicine intern will focus on the optimal number, length and angles of these segments. It is therefore necessary, that the angles of the cutting planes and the length of the defect can accurately be determined, resulting in the second objective:

- Develop a method to guide the saw blade using surgical navigation and evaluate the performance on the position and orientation of the cut, in comparison with the current 3D printed cutting guide.

After the position and orientation of the universal guide have been determined, the guide needs to be fixated so the surgeon is able to cut the mandible. This fixation should be sufficient to prevent any deviation of the planned cut, resulting in the third and final objective:

- Develop a method to fixate the navigated cutting guide to the mandible that allows for alterations, but is sufficient to prevent deviation from the surgical planning.

3 Registration in mandibular surgery

> *Clinically, registration is an important step in computer-assisted surgical navigation to correlate morphological information collected in different surgical stages, before, during and after the operation.*

3.1 Introduction

The current registration method at the NKI is not feasible for a navigated cutting guide. It would require the cutting guide to be placed before navigation is available, while navigation is needed for an accurate placement. Additionally, the intraoperative CT has a low resolution and takes OR time. Therefore a new registration method is preferred for the navigated cutting guide.

In literature, most methods utilise the teeth for registration of the mandible, maxilla or the entire skull [39, 44, 50–53]. The teeth are normally rigidly fixed inside the skull and can be viewed as an extension of the mandibular or maxillary bones. Teeth have been used as anatomical landmarks in the past [50], but are now mainly used as foundation for dental splints [39, 44, 51, 53]. However, OCC patients often have teeth problems and are either partially or completely edentate. Therefore, different registration methods alongside the dental splint need to be tested.

Artificial landmarks in the form of small screws can be placed under local anaesthesia before the operation during an outpatient visit. The patient would have a splint placed around the teeth or gingiva, and/or screws implanted before having a CT scan according to normal treatment procedures. This method results in a high quality preoperative scan with registration markers, without the additional patient dose and operation time of the intraoperative CT scan.

Widely spaced fiducials surrounding the target, result in the best registration [51, 54, 55]. However, this is not always possible in surgical oncology. Screws cannot be placed inside the tumour area, and must be placed surrounding or contralateral from the tumour. A study by Bettschart et al., maximised the fiducial spacing in a dental splint by creating an open mandible-maxilla splint [51]. This is difficult for oncological head and neck patients, as most suffer from trismus. These difficulties need to be taken into account for the fiducial placements of a registration method.

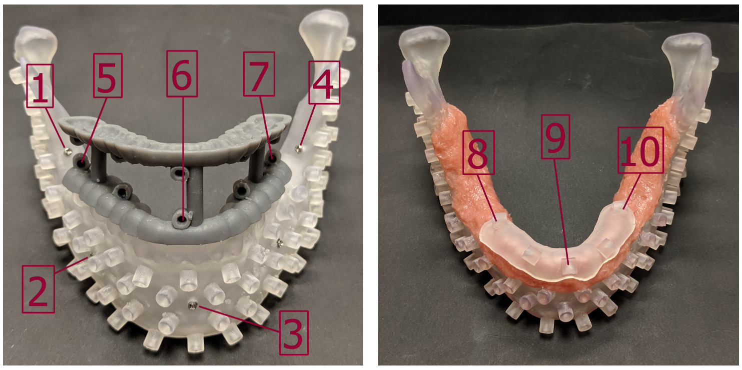

(a) Dentate mandible phantom **(b)** Edentate mandible phantom

Fig. 3.1: Dentate and edentate 3D printed phantom models with the corresponding registration splints. The used fiducial screws are numbered from 1 to 4, and the used fiducial pivots from 5 to 10.

Registration method	**Fiducials**
Screws	1-3-4
Screws contralateral	1-2-3
Screws + dental splint	1-3-7
Dental splint	5-6-7
Edentate splint	8-9-10

Tab. 3.1: The five different registration methods along with the fiducial combinations of Fig. 3.1

The goal is to determine the most optimal registration method for a navigated cutting guide. Therefore, in this phantom study, five registration methods are tested for mandibular registration, which do not require an intraoperative CT scan. These methods utilise screws, dental/gingiva splints with registration markers or a combination of these two as fiducials for registration. These fiducials are widely spaced surrounding or contralateral to the evaluated site. All methods are evaluated on accuracy and compared with the current golden standard of the NKI.

3.2 Method

3.2.1 Mandible phantom

To test the registration methods, phantom mandible models were created. Virtual generic dentate and edentate mandible models were edited using computer-assisted design freeware Meshmixer (Autodesk, Inc., `http://meshmixer.com`) and outfitted with evenly spread pivots made to fit the Aurora 6 degrees of freedom (DOF) probe. Thereafter, both phantoms were 3D printed using a Form 2 3D printer (Formlabs, Sommerville, Massachusetts, USA), using clear resin FLGPCL04. VST-50 Silicon Elastomer (Factor II, Inc., Lakeside, AZ, USA) was used to simulate the gingiva on the edentate mandible model. The dentate phantom was outfitted with five titanium screws 1.5x5mm Drill-Free maxDrive® (KLS Martin, Freiurg, Germany) in anatomically accessible positions in the mandible bone (Fig. 3.1). A dental and gingiva registration splint with pivots were made for the corresponding dentate and edentate phantoms. The edentate splint was printed using the same clear resin FLGPCL04, and the dentate splint using grey resin FLGPGR04. A CT scan with a 1mm slice thickness is made of both phantoms including the splints with the Siemens Somatom Sensation Open® (Siemens Medical Solutions, Erlangen, Germany).

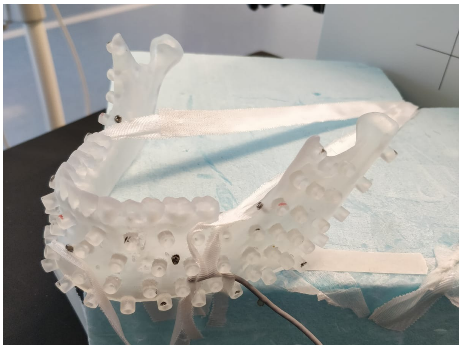

Fig. 3.2: Mandible phantom positioned in front of the NDI Planar electromagnetic field. The 6DOF sensor is secured on the lateral side.

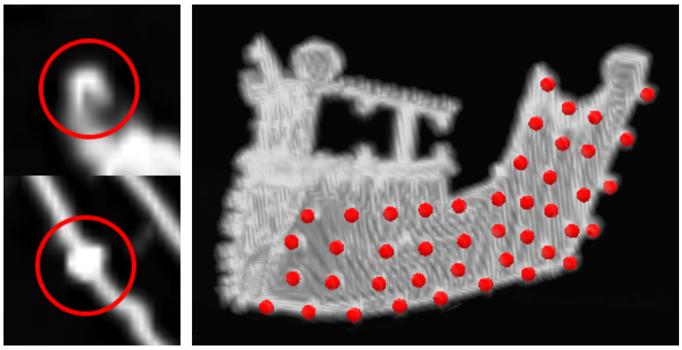

(a) Markers **(b)** Visualisation

Fig. 3.3: **(a)** Coronal CT slices of the phantom. Within the red circle the visibility of a registration pivot point is shown in the upper image. The lower image circles the visibility of a registration screw. **(b)** 3D visualisation of the dentate phantom with the 45 surface pivot points indicated in red spheres.

3.2.2 Registration procedure

To obtain realistic clinical accuracy, all registration methods are measured in an operating room. An Aurora planar field generator is mounted at the head of the OR-table. Following the current intraoperative procedure, a 6DOF EM sensor (Aurora 6DOF Cable Tool) is placed laterally on the outside of the mandible phantom (Fig. 3.2), the location where most tumours occur. The distance from the EM sensor to the field generator is 26 cm. In the red circles in figure 3.3a, a coronal CT slice of a pivot and screw are shown. The head of the registration screws or the centre of the pivots are manually marked within the CT scan using Surgnav, and denoted by ${}^{CT}\mathbf{p}_f$ with $f = \{1, 2, 3\}$. Thereafter, the Aurora 6DOF Probe is used to determine the position of the registration screws or pivots in the EM field, denoted by ${}^{EM}\mathbf{p}_f$. A registration to correlate the EM field to the CT scan can then be performed using the Procrustes algorithm. First the centres of gravity are calculated for both ${}^{CT}\mathbf{p}_f$ and ${}^{EM}\mathbf{p}_f$ as follows:

$$ {}^{CT}\bar{\mathbf{p}} = \frac{1}{3}\sum_{f=1}^{3} {}^{CT}\mathbf{p}_f \text{ and } {}^{EM}\bar{\mathbf{p}} = \frac{1}{3}\sum_{f=1}^{3} {}^{EM}\mathbf{p}_f \tag{3.1} $$

Translational differences are eliminated by translating both centres of gravity to the origin.

$$ \text{For all } f: \begin{array}{c} {}^{CT}\breve{\mathbf{p}}_f = {}^{CT}\mathbf{p}_f - {}^{CT}\bar{\mathbf{p}} \\ {}^{EM}\breve{\mathbf{p}}_f = {}^{EM}\mathbf{p}_f - {}^{EM}\bar{\mathbf{p}} \end{array} \tag{3.2} $$

The rotation matrix ${}^{CT}\hat{\mathbf{R}}_{EM}$ to transform EM data to CT data is calculated using Kabsch algorithm with $3 \times F$ matrices $\mathbf{A}$ and $\mathbf{B}$ containing points ${}^{CT}\breve{\mathbf{p}}_f$ and ${}^{EM}\breve{\mathbf{p}}_f$, where the singular values $\mathbf{U}, \mathbf{S}$ and $\mathbf{V}$ are found such that:

$$\mathbf{USV}^T = \mathbf{AB}^T \tag{3.3}$$

$${}^{CT}\hat{\mathbf{R}}_{EM} = \mathbf{UV}^T \tag{3.4}$$

Lastly, the translation vector ${}^{CT}\hat{\mathbf{t}}_{EM}$ can be calculated as follows:

$${}^{CT}\hat{\mathbf{t}}_{EM} = {}^{CT}\bar{\mathbf{p}} - {}^{CT}\hat{\mathbf{R}}_{EM}{}^{EM}\bar{\mathbf{p}} \tag{3.5}$$

For the surface pivot points around the tumour region, as shown in figure 3.3b, both the CT scan locations denoted by ${}^{CT}\mathbf{r}_n$, and Aurora probe locations denoted by ${}^{EM}\mathbf{m}_n$, with $n = \{1, 2, ..., 45\}$ for the dentate model, and $n = \{1, 2, ..., 35\}$ for the edentate model, are acquired in the same method as the registration points. Where the measured points of the Aurora probe are cast from EM coordinates to CT coordinate to facilitate later analyses:

$${}^{CT}\mathbf{m}_n = {}^{CT}\hat{\mathbf{R}}_{EM}{}^{EM}\mathbf{m}_n + {}^{CT}\hat{\mathbf{t}}_{EM} \tag{3.6}$$

This method is repeated five times for each of the five registration point combinations (Tab. 3.1 and Fig. 3.1).

3.2.3 Analyses

The Target Registration Error (TRE) is the difference between the reference ${}^{CT}\mathbf{r}_n$ and measured ${}^{CT}\mathbf{m}_n$ position of the surface pivots. This difference between two 3D points can be evaluated as the Euclidean distance, which is the straight-line distance between two points. This distance and thus the TRE can be calculated as the square root of the sum of squared deviations in all three spatial directions:

$$\text{For all } n : TRE_n = \sqrt{(x_{m,n} - x_{r,n})^2 + (y_{m,n} - y_{r,n})^2 + (z_{m,n} - z_{r,n})^2} \tag{3.7}$$

To visualise the accuracy of the registration, the TRE is mapped onto a 3D surface model of the mandible, using colour coding.

Last, the root mean square error (RMSE) is calculated, to compare the accuracy of the registration method with the current method used in the NKI. The RMSE is calculated per registration method, and is defined as the square root of the average of all squared TRE, with $N = 45$ for the dental model and $N = 35$ for the edentate model.

$$RMSE = \sqrt{\frac{\sum_{n=1}^{N}(TRE_n)^2}{N}} \tag{3.8}$$

The square of the errors causes larger errors to have a disproportionately large effect on RMSE.

3.2.4 Statistical analysis

Quantile-quantile plots of the variation in the TRE between the different registration methods determined that the data were not normally distributed. A Kruskal-Wallis H test was used to examine whether there was a significant difference between the methods. Bonferroni corrected Dunn's posthoc tests were used to identify any significant differences between each pair following Kruskal-Wallis H analysis. The difference was considered significant if the probability value (p) was less than 0.05 in SPSS version 25.0 (IBM, Armonk, NY, USA).

3.3 Results

The registration steps were fast and easy to perform; it took less than a minute. Kruskal-Wallis H test showed that there were statistically significant differences between the different registration methods. Dunn's pairwise tests showed that there was a statistical difference between the dental splint and all other methods ($p < 0.001$), and statistical differences between the screws contralateral and all other methods ($p < 0.001$). There was no statistical difference between screws, screws + dental splint or the edentate splint ($p > 0.196$). The dental splint registration method had the lowest RMSE, min and max TRE of all the registration methods (Tab. 3.2). The regional accuracy after registration is demonstrated by mapping the average TRE of the repeated measurement onto a virtual 3D model of the mandible, using colour coding (Fig. 3.4).

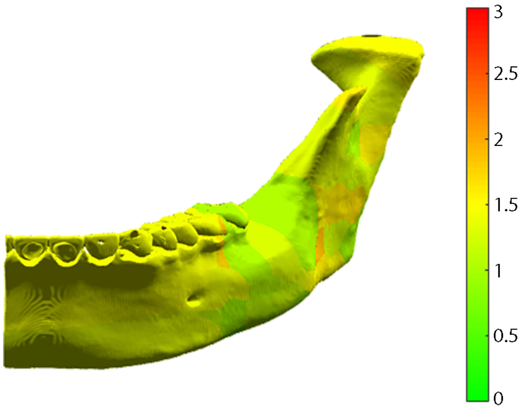

(a) Screws

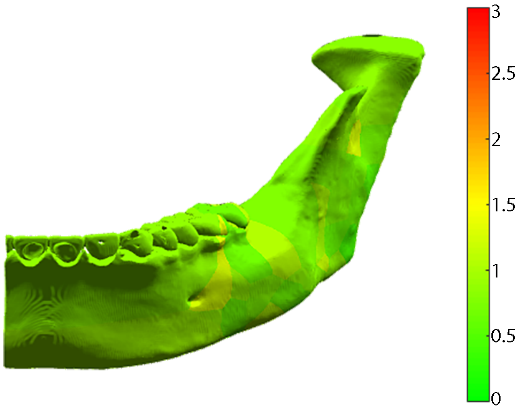

(d) Dental splint

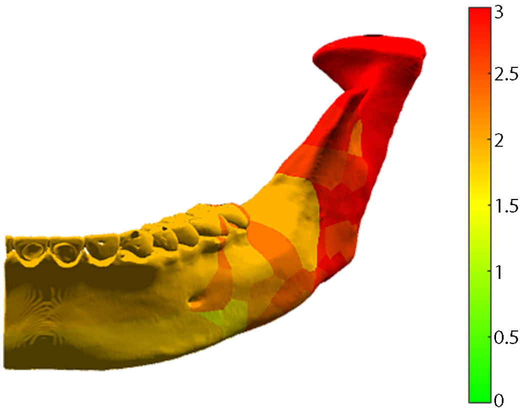

(b) Screws contralateral

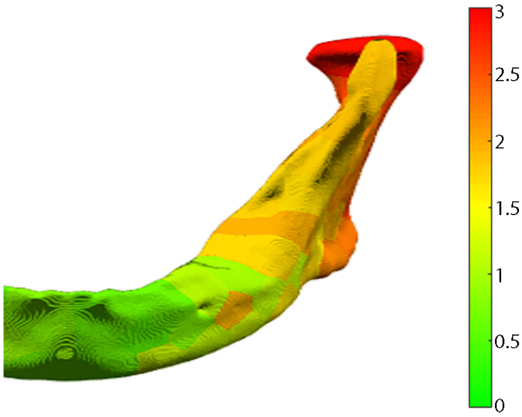

(e) Edentate splint

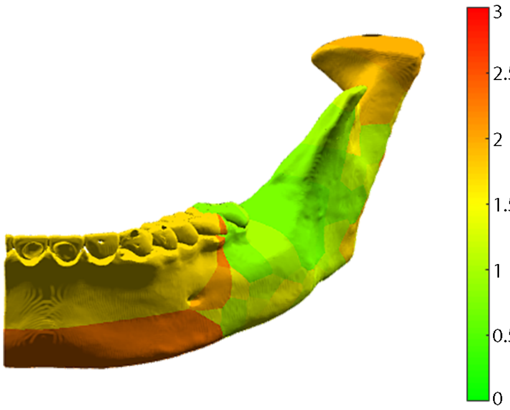

(c) Screws + dental splint

Registration method	Target registration error (mm)		
	RMSE	Min	Max
Screws	1.35	0.10	2.49
Screws contralateral	2.81	0.92	6.51
Screws + dental splint	1.45	0.33	3.13
Dental splint	0.89	0.15	2.05
Edentate splint	1.95	0.25	4.16

Tab. 3.2: TRE average, minimum and maximum results of the four different registration methods, using 45 surface points for the dentate model and 35 surface points for the edentate model.

Fig. 3.4: The regional accuracy after registration, demonstrated by mapping the average TRE of the repeated measurement onto a virtual 3D model of the mandible, using colour coding. The colourbar ranges from 0 mm (green) to 3 mm (red).

3.4 Discussion

The current registration method at the NKI is impractical for a navigated cutting guide. Therefore, five different registration methods utilising splints, screws or a combination are evaluated. The goal was to find a registration method which is on par or better than the current registration method of the NKI. In a previous graduation thesis the accuracy of this registration method was evaluated on six patients, were an RMSE was calculated for each patient resulting in an average of 2.1 mm with a maximum of 3.7 mm and a minimum of 1.4 mm [49].

In this study, registration using the dental splint had the lowest TRE and was statistically better than all the other registration methods. Registration with the contralateral screws is the only method with a RMSE higher than 2 mm, marking it as undesirable. The other registration methods using screws performed much better, an explanation could be that the contralateral screws are placed closer together and/or that the centre of gravity of the screws is further from the target [55]. The edentate splint with a RMSE of 1.95 mm is just below the 2.1 mm threshold, showing that it could potentially be used as a substitute registration method. However, the 4.16 mm maximum value is still high when compared with the normal 10 mm surgical margin. The screws-only registration method is a good alternative for edentate patients. The RMSE of 1.35 mm is well below the 2.1 mm threshold, and the screws can also be placed in edentate patients. The only downside of this registration method is the invasive placement of the screws. However, patients who require surgical navigation, already undergo major surgery. The minimal invasiveness of the screw placement is thus of little concern.

The large difference between the screws-only and the dental splint method was not expected. The screws are directly drilled into the model, while the dental splint is a secondary object placed upon the teeth of the model. It was expected that movement or inaccurate placing would make the dental splint inferior to the screws-only method. Literature using the same navigation system [39] or optical navigation [51], use a dental splint made from resin incorporated with titanium screws. Their achieved results are comparable with the screws-only registration method of this study. This could imply that the titanium screws were the limiting factor. Visibility of the screw head in the CT was sometimes difficult, while the cone shaped pivots were easier to identify. If the manually selected location of the screw heads in the CT is wrong, this impacts the entire registration. An automatic method for finding the screw heads, such as template matching, could improve the results. Pivot points could also be implemented to fit on the screw heads, and thus increase their visibility.

The registration screws/pivots and the surface pivots are all manually selected by a single observer. A different observer could obtain slightly different results. All measurements were performed inside the OR, but with stationary phantom models. Further clinical tests are required before implementation can be advised. The dental splint was created using the 3D model of the dental phantom, resulting in a near perfect fit. In a patient study, a 3D model of the teeth can be obtained using an intraoral scanner [56]. A next step could be to compare the dental splint with the current registration method during surgery.

3.5 Conclusion

In this phantom study, five different registration methods utilising screws, splints or a combination, were evaluated as replacements for the current registration method at the NKI; the intraoperative cone beam CT. The dental splint had the highest registration accuracy, showing a clear improvement on the current registration method of the NKI. For edentate patients, the non-invasive edentate splint had an accuracy comparable with the current registration method. However, registration utilising widely spaced screws near the target site had a much higher accuracy. The patient will already undergo major surgery, making the screws invasiveness negligible. Further research is required to evaluate the accuracy in a clinical setting.

Navigated surgical cutting guide

4

> *In mechanical usage, a guide is something that steadies or directs the motion of an object*

4.1 Introduction

Recently, two research groups have been working on a navigated saw for performing virtually-planned mandibular osteotomies [46, 47]. The implementation of the navigated saw can be carried out exclusively by in-house OR personnel, thereby eliminating the need for external bioengineer services, and the relatively long production and design time of the 3D printed cutting guides [47, 57].

In an experimental setting, multiple osteotomies were performed on plaster or polyurethane model mandibles. Pietruski et al. [47] let a single operator perform the osteotomies and two observers evaluate the difference in volume, the angular deviations and the difference between preoperative and postoperative marginal point positions. The mean difference between the planned and actual bone resection volumes was 8.55 ± 5.51%, the mean angular deviation between planned and actual osteotomy trajectory was 8.08 ± 5.50°, and the mean difference between the preoperative and the postoperative marginal point positions was 2.63 ± 1.27 mm [47]. The study highlights the potential for image-guided resection, but the method requires further improvement and a comparison with the patient specific 3D printed cutting guides. Bernstein et al. [46] let four surgeons (two attending, two clinical fellows) perform unnavigated and navigated osteotomies and evaluated the distance and angular deviations (here, pitch and roll) between the planned and the cutting planes. The navigated cuts were significantly better than the unnavigated cuts in all evaluated measures. Mean distance from the virtual plan was 2.65 ± 2.25 mm unnavigated and 1.3 ± 0.80 mm 3D navigated; mean pitch was 5.06 ± 4.24° unnavigated and 4.11 ± 2.72° 3D navigated; mean roll was 9.4 ± 8.3° unnavigated and 3.5 ± 3.1° 3D navigated. However, no comparison is made with the patient specific cutting guides.

Both of these groups show the potential of surgical navigation in providing accurate osteotomies, but using a free-hand navigated saw requires good eye-hand coordination [47] and without a saw-compelling cutting guide it is possible to make a non-straight cut. These studies achieved a good accuracy in distance, but still have high angular deviations. During reconstruction, this deviation works over the entire length of the defect and can thus result in a large effect.

The aim of this study was to assess the accuracy and reproducibility of 3D virtually-planned osteotomies in mandible models using a novel EM navigated surgical cutting guide and to compare the results with our current state-of-the-art patient specific 3D printed cutting guides and the experimental navigated saws as found in literature.

4.2 Method

4.2.1 Plaster Mandibles

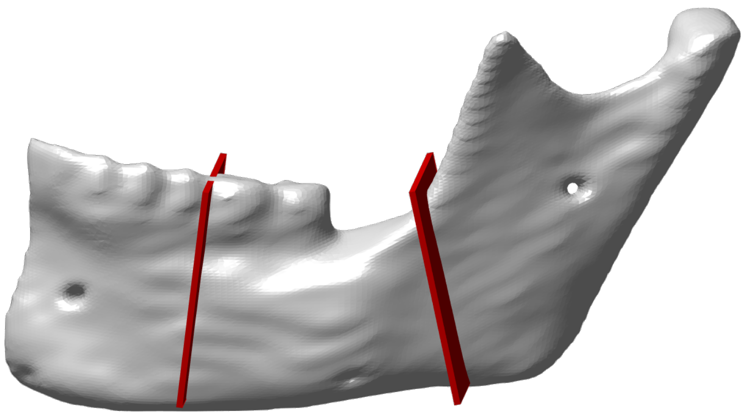

Fig. 4.1: 3D model of the plaster mandible with the planned osteotomies indicated in red.

A virtual generic dentate mandible model was split along the midsagittal plane, where the left half was used to create a mold. Using this mold, ten plaster mandible models were created using generic plaster. All of the plaster models were scanned individually using a CT (Somatom Sensation Open; Siemens Medical Solutions, Erlangen, Germany) with a resolution of 0.59 mm/pixel and a 1.5 mm slice thickness. The segmentation of the plaster mandibles was performed with the 3D Slicer software platform [58] using a simple threshold. Using computer-assisted design freeware Meshmixer (Autodesk, Inc., http://meshmixer.com), two osteotomies based on actual cases of osteotomy locations were planned and drawn in 3D for each plaster mandible model (Fig 4.1).

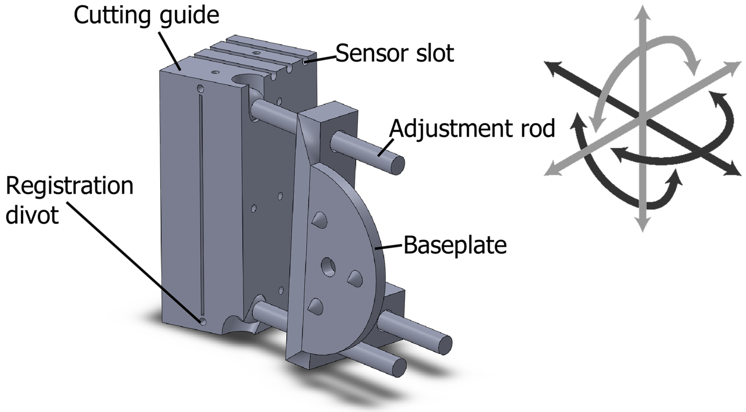

Fig. 4.2: 3D model of the navigated cutting guide, dubbed "Bladerunner". In the upper right corner, displayed in black are the 3 degrees of freedom.

4.2.2 Bladerunner

An experimental navigated cutting guide system (dubbed Bladerunner) was designed consisting of three elements; a baseplate for a rigid fixation to the mandible, a navigated cutting guide and adjustment rods (Fig. 4.2). The baseplate has three equidistant spikes with a screw hole in the center to provide the best kinematic constraint on an irregular surface such as the mandible, and a L-shaped support with three holes for the adjustment rods. The connection and mobility provided by the adjustment rods is derived from a kinematic mirror mount, to provide 3DOF movement. By elongating or shortening the adjustment rods, the navigated cutting guide is able to rotate and translate opposed to the baseplate. This is necessary for providing minute and larger adjustment options to obtain the best positioning according to planning. When the optimal position and orientation is obtained the setup can be fixed using opposing nuts along the adjustment rods. The navigated cutting guide has a 30x20x1mm slit to adequately compel the saw, a trench for the EM sensor and fourteen widely spaced indentations on the outer surface which can be used for registration. The prototype was 3D printed on a Formlabs Form 2 stereolithographic printer (Formlabs, Somerville, USA) using clear resin FLGPCL04.

4.2.3 Registration

To obtain realistic clinical accuracy all procedures are performed in a real OR setting. EM sensors were attached with tape in between the two osteotomies on the plaster models, and in the specifically designed groove of the Bladerunner. The Bladerunner and the plaster jaws were both registered using a point match registration. The plaster mandible models were registered to the 3D models with the virtual planning using three widely spaced fiducials drilled into the models. Image-to-sensor paired-point registration was measured in the RMSE to assess how closely the preoperative CT and physical plaster jaw model were registered. The Bladerunner was registered to the 3D model using fourteen widely spaced fiducials in the form of small indentations along its surface.

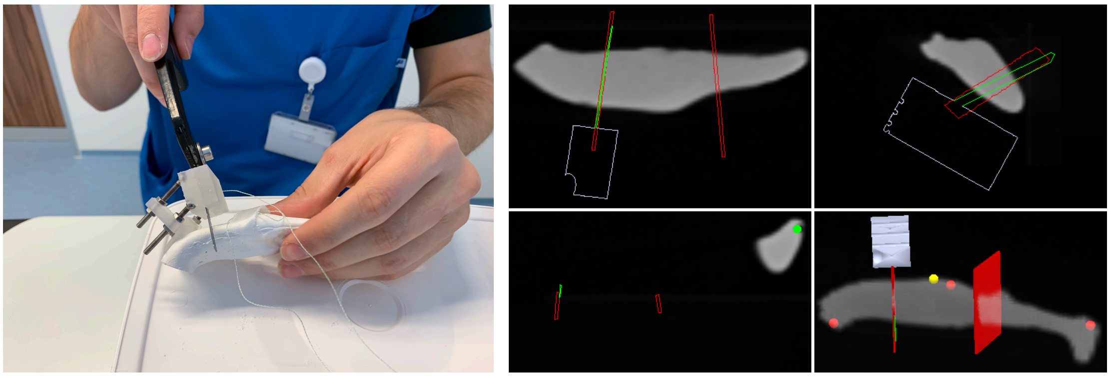

(a) Performing the osteotomy

(b) Positioning the Bladerunner using Surgnav

Fig. 4.3: An osteotomy being performed on a plaster mandible model using the 3D navigated cutting guide in combination with Surgnav and a 0.1 mm thin handheld hacksaw.

4.2.4 Osteotomies

The baseplate was attached to the plaster jaw using a stainless steel screw. Next, the Bladerunner was positioned using the 3D views of SurgNav in such a way that the predicted cutting plane was superimposed on the planned osteotomy (Fig 4.3b). Rigid fixation was attained by tightening opposing nuts on the adjustment rods. A 0.1 mm thin handheld hacksaw was inserted through the Bladerunner and used to perform the osteotomies (Fig 4.3a). All mandibular osteotomies were made subtotal (approximately 80% of the cut height) so that each mandible model remained intact and could be scanned whole to facilitate the analysis.

4.2.5 Osteotomy analyses

After completing the osteotomies, the mandible models scanned in a CT with identical imaging parameters to the preoperative scans. Segmentations were again performed with 3D Slicer using the same threshold value. Both pre- and postoperative segmentations were registered in MATLAB R2018b (The MathWorks Inc., Natick, USA) using an Iterative Closest Point (ICP) algorithm. Model-to- model registration error was determined as the RMSE between the planned and registered models, to confirm the accuracy of the quantitative outcome measures. Points on the surface of the osteotomy were determined by finding opposing outward orientated normal vectors, where the corresponding vertices had an intermediate distance equal to the thickness of the osteotomy. Resection planes were defined by determining a plane of best fit through these points by minimizing the normal quadratic distance. Distance

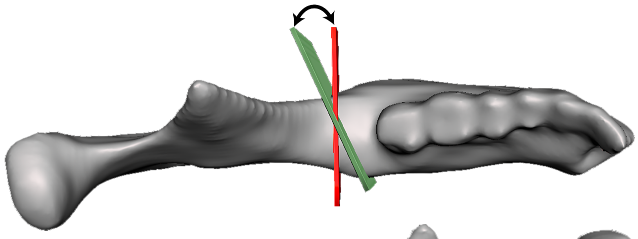

(a) Yaw

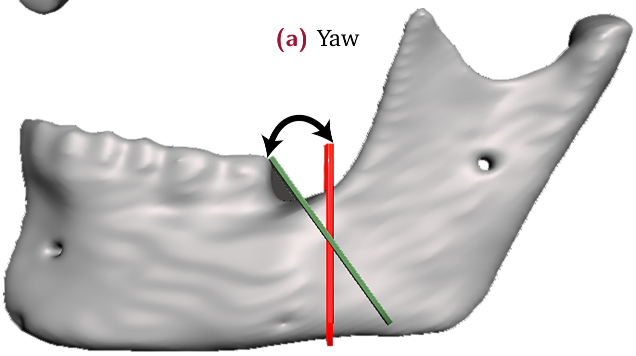

(b) Roll

Fig. 4.4: Visual representation of the deviation in orientation between the planned and performed osteotomy.

between the planned and postoperative resection plane was defined as the distance between the centres of gravity of each plane intersected with the preoperative model. Both planes were transformed to align the planned resection plane along the Z-axis, before performing a registration to determine the yaw and the roll between the planes (Fig. 4.4).

4.2.6 Statistical analysis

To compare the results of the navigated cutting guide with those of the current state-of-the-art 3D printed cutting guide and the navigated saw, data from other sources have been obtained. The 3D printed cutting guide data consist of preliminary data from a study into the performance of the 3D printed cutting guide, which included seven patients at the moment of comparison [59]. Bernstein et al. [46] provided a dataset in their article of unnavigated and navigated maxillary and mandibular osteotomies, where only the mandibular osteotomies were used for this comparison. The unnavigated osteotomies were only used as a reference and not included in the statistical analysis. Quantile- quantile plots of the variation in the distance, yaw, and roll between the planned and performed osteotomies determined that the data were not normally distributed. A Kruskal-Wallis H test was used to examine whether there was a significant difference between the navigated groups. Bonferroni corrected Dunn's posthoc test was used to identify any significant difference between each pair following Kruskal-Wallis H analysis. The difference was considered significant if the p-value was less than 0.05 in SPSS version 25.0 (IBM, Armonk, NY, USA).

Method (no. of osteotomies)	Distance (mm)				Yaw (deg)				Roll (deg)			
	Median	Q1	Q3	IQR	Median	Q1	Q3	IQR	Median	Q1	Q3	IQR
Unnavigated (144)	2,1	1,1	3,6	2,5	3,9	2,1	6,9	4,8	7,3	4,4	11,5	7,1
3D navigated Saw (144)	1,2	0,6	1,7	1,1	3,7	2	5,7	3,7	2,6	1,3	5,2	3,9
Cutting Guide (13)	1,3	0,6	1,9	1,3	3,5	0,7	9,5	8,8	3,6	1,4	5,0	3,6
3D navigated Bladerunner (20)	1	0,7	1,4	0,7	1,6	0,7	3,2	2,5	1,1	0,5	2,6	2,1

Tab. 4.1: Differences in distance, yaw and roll between the virtually planned osteotomy and the performed osteotomies. Abbreviations: deg, degrees; IQR, interquartile range; Q1, first quartile upper boundary; Q3, third quartile upper boundary.

4.3 Results

A total of 20 osteotomies guided with the Bladerunner were performed on ten plaster mandible models. Kruskal-Wallis H tests with the 3D navigated saw, 3D navigated Bladerunner and the cutting guide showed that there were statistically significant differences in yaw ($p = 0.001$) and roll ($p = 0.013$) but not in distance ($p = 0.640$). Dunn's pairwise tests were carried out for yaw and roll in the three pairs of groups. In the yaw, there were statistically significant differences between the Bladerunner with the saw ($p < 0.001$) and with the cutting guide ($p = 0.035$). In the roll, there were statistically significant differences between the Bladerunner with the saw ($p = 0.018$) and with the cutting guide ($p = 0.043$). There were no significant differences between the navigated saw and the cutting guide. The median values and IQRs were smallest in the 3D navigated Bladerunner osteotomies (Tab. 4.1, Fig. 4.5).

The median image-to-sensor paired-point registration error was 0.4 mm (IQR 0.4 mm) and the median model-to-model registration error was 1.0 mm (IQR 0.1 mm).

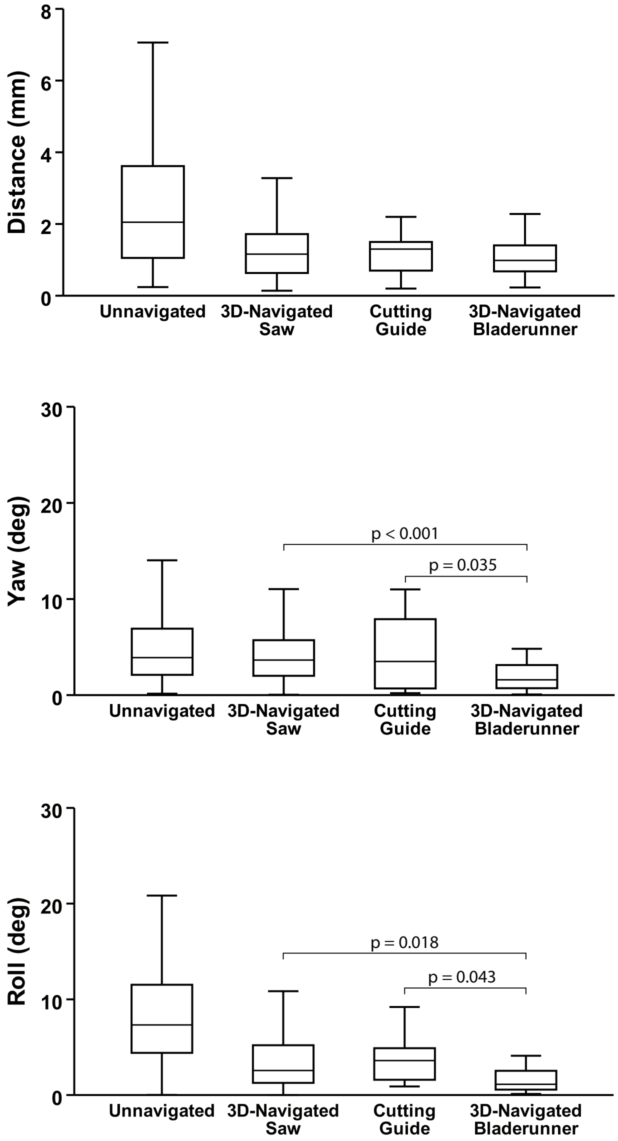

Fig. 4.5: Box-and-whisker plots showing the distance, yaw and roll of the unnavigated and 3D navigated osteotomies. Bars denote median, boxes show interquartile range (IQR), upper whiskers show third quartile plus 1.5 IQR, and lower whiskers show first quartile minus 1.5 IQR.

4.4 Discussion

The current state-of-the-art 3D printed cutting guides have shown to be a clear improvement on the old free-hand techniques. However, these cutting guides come with their own shortcomings in the form of inflexibility during surgery, long production time and cost. Several research groups have started to look for alternative methods in the form of a navigated saw. In this study the concept of a navigated cutting guide is introduced and multiple navigated osteotomies were performed to evaluate the efficacy.

The navigated Bladerunner has the smallest median values and IQRs, indicating that it has the highest accuracy and reproducibility. Furthermore, both the yaw and the roll are significantly better than the navigated saw and the 3D printed cutting guide. With a p value of 0.640, there was no statistically improvement in the distance, but the distance does not have much to be gained. The difference between 2 and 1 mm is clinically less relevant than the multiple degree improvements of the yaw and the roll. These angles work over the entire arm of the reconstruction, a small deviation in angle can result in a multiple millimetre offset over the length of the reconstruction. The yaw and roll is where the Bladerunner provides improvement.

Both navigated saw groups [47, 51] utilise an optical navigation system, as EM navigation has demonstrated to be inaccurate in the vicinity of large metallic instruments such as the saw [60] or OR-table. However, surgical navigation with a navigated cutting guide is only needed during the actual positioning of the Bladerunner, at this point no interfering metallic instruments are needed. After the correct position and orientation is obtained, the navigation system can even be turned off without impacting the osteotomy. When using optical navigation, the required line-of-sight between the optical tracker and surgical tools limits the surgeons flexibility and is difficult to guarantee in practice, especially in small working areas like in head and neck surgery [39]. Therefore, EM navigation is the preferred system for the navigation of the navigated cutting guide.

The benefit of a navigated cutting guide versus a navigated saw, is that the guide compels the saw, making a curved cut impossible. The free-hand navigated saw requires good eye-hand coordination during the positioning and performing the osteotomy which could impact the performance [51]. The navigated cutting guide only requires this eye-hand coordination during positioning. When the cutting guide is aligned according to planning, the position of the Bladerunner can be fixed so the surgeon can focus on performing the osteotomy.

This study is still only a proof of concept and thus has some limitations. The Bladerunner setup requires that the baseplate is attached to the mandible at some distance from the planned osteotomy. As it is not feasible to position the baseplate on the tumour site, it is currently difficult to perform an osteotomy near the condyle of the mandible. In further studies this could be alleviated by providing multiple baseplates for different attachment locations. The fixation of the Bladerunner is achieved by tightening opposing bolts on the adjustment rods. While this was fine for the proof of concept, this is not feasible during surgery. Different fixation options are required, which also provides room for improvement. If the turning of the adjustment rods can be measured in strokes during positioning, the surgical navigation software can interactively provide the surgeon with the required turning strokes per rod, to achieve the best positioning according to planning. This could decrease the error introduced by the user, reducing the inter-user variability.

Future studies will try to incorporate the previously stated improvements and asses the technology in a clinical patient study.

4.5 Conclusion

This study shows the potential for a navigated cutting guide for mandibular osteotomies. The distance, yaw, and roll were accurate and had a high reproducibility. Despite the initial stage of this research, a statistically significant improvement is seen in the angles of the performed osteotomies. Future steps will include improvements to the navigated cutting guide setup and a clinical patient study.

5 Overall Conclusion

The current 3D printed cutting guides for mandibular osteotomies do not allow for alterations of the preoperative planning and has a lengthy time interval between planning and surgery. Additionally, the current registration method using intraoperative cone beam CT takes OR time and has a low resolution. The aim of this study was to develop a surgical navigation procedure for mandibular surgery and evaluate its feasibility and accuracy, to provide guidance during and decrease the delay before surgery.

Intraoperative registration methods using screws and dental/gingiva splints have been evaluated for head and neck surgery. These methods translate the virtual surgical planning to the OR without the need for intraoperative imaging. In this phantom study, similar and better results compared to the clinical cone beam CT registration were achieved.

A navigated cutting guide has been developed which can be fixated to the mandible and adjusted to conform to the surgical planning. The guide has been tested on multiple plaster mandible models, and evaluated on the accuracy of the position and orientation of the osteotomies. The accuracy of the position was similar to that of the 3D printed cutting guide and a navigated saw found in literature. The accuracy of the orientation was significantly better than both the 3D printed cutting guide and the navigated saw.

6 Future perspectives

As all measurements performed in this study have been done using phantom models, the next step towards clinical implantation is clinical testing. In a future study, the patients teeth, and gingiva can be imaged using the 3Shape TRIOS® Intraoral Scanner currently available in the NKI. Whereupon the 3D model obtained from this scan can be used to create a patient-specific splint. During the surgery the registration should be performed using both the intraoperative CT and the splints/screws method, and evaluated on the same points. This will give an accurate comparison of the two methods in a clinical setting.

The navigated cutting guide study has shown the potential for the Bladerunner in mandibular osteotomies. However, with adjustments, the Bladerunner could also be used for osteotomies in other anatomical sites such as the maxilla or even the knee and hip. The design still has room for improvement, but the results are already very promising. Clinical testing is also required, after the previously mentioned improvements have been made regarding the mandibular attachment and the fixation of the adjustment rods. The splints/screws registration would be the preferred registration method, if the registration clinical tests prove that they are a valid alternative. Otherwise, the current intraoperative cone beam CT registration can still be used, but it would limit the placement of the Bladerunner. The baseplate would need to be attached to the mandible to provide the intraoperative CT with artificial landmarks for a good registration. The splints/screws method would not have this issue, as registration can be performed using the artificial landmarks of the splint or screws.

For the reconstruction after mandibular osteotomies, it is necessary to be able to translate the position and orientation of the performed mandibular osteotomies to fibular segments. If there was an adjustment to the mandibular planning, this needs to follow into adjustments to the fibula planning. A (semi-)automatic fibula planning is required which calculates the optimal number, length and angles of the fibula segments to reconstruct the defect left by the performed osteotomies.

Bibliography

[1] G. Breeland and B. C. Patel. *Anatomy, Head and Neck, Mandible*. StatPearls Publishing, Nov. 2019. URL: http://www.ncbi.nlm.nih.gov/pubmed/30335325 (cit. on p. 1).

[2] H. Basit, B. J. Eovaldi, and M. A. Siccardi. „Anatomy, Head and Neck, Mastication Muscles". In: (May 2019). URL: https://www.ncbi.nlm.nih.gov/books/NBK541027/ (cit. on p. 1).

[3] H. Gray. *Anatomy of the Human Body*. 20th ed. Philadelphia and New York, 1918. URL: https://www.bartleby.com/107/ (cit. on p. 1).

[4] R. Sarkar. „Pathological and clinical features of primary osseous tumours of the jaw". In: *Journal of Bone Oncology* 3.3-4 (Nov. 2014), pp. 90–95 (cit. on p. 2).

[5] L. P. Rao, S. R. Das, A. Mathews, et al. „Mandibular invasion in oral squamous cell carcinoma: Investigation by clinical examination and orthopantomogram". In: *International Journal of Oral and Maxillofacial Surgery* 33.5 (2004), pp. 454–457 (cit. on pp. 2, 3).

[6] Integraal kankercentrum Nederland. *Nederlandse Kankerregistratie - cijfers over kanker*. URL: https://www.cijfersoverkanker.nl/ (visited on Oct. 5, 2018) (cit. on p. 2).

[7] F. Bray, J. Ferlay, I. Soerjomataram, et al. „Global cancer statistics 2018: GLOBOCAN estimates of incidence and mortality worldwide for 36 cancers in 185 countries." In: *CA: A Journal for Clinicians* 00.00 (Sept. 2018), pp. 1–31. arXiv: arXiv:1011.1669v3 (cit. on p. 2).

[8] C. S. Farah, M. Jessri, S. Currie, et al. „Aetiology of Oral Cavity Cancer". In: *Contemporary Oral Oncology*. Cham: Springer International Publishing, 2017, pp. 31–76 (cit. on p. 2).

[9] N. W. Johnson, B. Gupta, A. Ariyawardana, and H. Amarasinghe. „Epidemiology and Site-Specific Risk Factors for Oral Cancer". In: *Contemporary Oral Oncology: Biology, Epidemiology, Etiology, and Prevention*. Cham: Springer International Publishing, 2017, pp. 103–153 (cit. on p. 2).

[10] J. Bagan, G. Sarrion, and Y. Jimenez. „Oral cancer: Clinical features". In: *Oral Oncology* 46.6 (June 2010), pp. 414–417 (cit. on p. 2).

[11] V. Ernani and N. F. Saba. „Oral Cavity Cancer: Risk Factors, Pathology, and Management". In: *Oncology* 89.4 (2015), pp. 187–195 (cit. on p. 2).

[12] M. Pogrel, B. Schimidt, and C. Robertson. „Clinical Pathology : Odontogenic and nonodontogenic tumors of the Jaws“. In: *Oncology* (2006), pp. 490–534 (cit. on pp. 2, 3).

[13] A. L. Weber, C. Bui, and T. Kaneda. „Malignant tumors of the mandible and maxilla“. In: *Neuroimaging Clinics of North America* 13.3 (Aug. 2003), pp. 509–524 (cit. on p. 2).

[14] D. N. Sutton, J. S. Brown, S. N. Rogers, E. D. Vaughan, and J. A. Woolgar. „The prognostic implications of the surgical margin in oral squamous cell carcinoma“. In: *International Journal of Oral and Maxillofacial Surgery* 32.1 (2003), pp. 30–34 (cit. on pp. 2, 3).

[15] Breast Cancer Care. *Surgery to treat breast cancer*. URL: `https://www.breastcancercare.org.uk/information-support/facing-breast-cancer/going-through-treatment-breast-cancer/surgery` (visited on Oct. 9, 2018) (cit. on p. 3).

[16] M. Alicandri-Ciufelli, M. Bonali, A. Piccinini, et al. „Surgical margins in head and neck squamous cell carcinoma: What is 'close'?“ In: *European Archives of Oto-Rhino-Laryngology* 270.10 (2013), pp. 2603–2609 (cit. on p. 3).

[17] R. W. Nason, A. Binahmed, K. A. Pathak, A. A. Abdoh, and G. K. Sándor. „What is the adequate margin of surgical resection in oral cancer?“ In: *Oral Surgery, Oral Medicine, Oral Pathology, Oral Radiology and Endodontology* 107.5 (2009), pp. 625–629 (cit. on p. 3).

[18] M. Bak, A. S. Jacobson, D. Buchbinder, and M. L. Urken. „Contemporary reconstruction of the mandible“. In: *Oral Oncology* 46.2 (2010), pp. 71–76 (cit. on p. 4).

[19] B. P. Kumar, V. Venkatesh, K. A. J. Kumar, B. Y. Yadav, and S. R. Mohan. „Mandibular Reconstruction: Overview“. In: *Journal of Maxillofacial and Oral Surgery* 15.4 (Dec. 2016), pp. 425–441 (cit. on pp. 3, 4).

[20] J. S. Brown, D. Lowe, A. Kanatas, and A. Schache. „Mandibular reconstruction with vascularised bone flaps: a systematic review over 25 years“. In: *British Journal of Oral and Maxillofacial Surgery* 55.2 (2017), pp. 113–126. URL: `http://dx.doi.org/10.1016/j.bjoms.2016.12.010` (cit. on p. 3).

[21] K. A. Hurvitz, M. Kobayashi, and G. R. Evans. „Current options in head and neck reconstruction“. In: *Plastic and Reconstructive Surgery* 118.5 (2006), pp. 122–133 (cit. on p. 3).

[22] M. Rana, R. Warraich, H. Kokemüller, et al. „Reconstruction of mandibular defects - Clinical retrospective research over a 10-year period - Clinical r“. In: *Head and Neck Oncology* 3.1 (Apr. 2011), p. 23 (cit. on p. 4).

[23] J. L. Williams. „Reconstruction of mandibular defects“. In: *International Journal of Oral Surgery* 2.5 (May 1973), pp. 167–178 (cit. on p. 4).

[24] R. E. Hayden, D. P. Mullin, and A. K. Patel. „Reconstruction of the segmental mandibular defect: Current state of the art“. In: *Current Opinion in Otolaryngology and Head and Neck Surgery* 20.4 (2012), pp. 231–236 (cit. on p. 4).

[25] R. C. W. Wong, H. Tideman, L. Kin, and M. A. W. Merkx. „Biomechanics of mandibular reconstruction: a review“. In: *International Journal of Oral and Maxillofacial Surgery* 39.4 (2010), pp. 313–319 (cit. on p. 4).

[26] S. Mazzoni, C. Marchetti, R. Sgarzani, et al. „Prosthetically guided maxillofacial surgery: Evaluation of the accuracy of a surgical guide and custom-made bone plate in oncology patients after mandibular reconstruction“. In: *Plastic and Reconstructive Surgery* 131.6 (2013), pp. 1376–1385 (cit. on pp. 4, 5).

[27] G. Succo, M. Berrone, B. Battiston, et al. „Step-by-step surgical technique for mandibular reconstruction with fibular free flap: Application of digital technology in virtual surgical planning“. In: *European Archives of Oto-Rhino-Laryngology* 272.6 (June 2015), pp. 1491–1501 (cit. on p. 4).

[28] B. D. Foley, W. P. Thayer, A. Honeybrook, S. McKenna, and S. Press. „Mandibular reconstruction using computer-aided design and computer-aided manufacturing: An analysis of surgical results“. In: *Journal of Oral and Maxillofacial Surgery* 71.2 (2013), e111–e119 (cit. on p. 4).

[29] A. Modabber, C. Legros, M. Rana, et al. „Evaluation of computer-assisted jaw reconstruction with free vascularized fibular flap compared to conventional surgery: A clinical pilot study“. In: *International Journal of Medical Robotics and Computer Assisted Surgery* 8.2 (June 2012), pp. 215–220 (cit. on p. 4).

[30] K. A. Rodby, S. Turin, R. J. Jacobs, et al. „Advances in oncologic head and neck reconstruction: Systematic review and future considerations of virtual surgical planning and computer aided design/computer aided modeling“. In: *Journal of Plastic, Reconstructive and Aesthetic Surgery* 67.9 (2014), pp. 1171–1185. URL: `http://dx.doi.org/10.1016/j.bjps.2014.04.038` (cit. on p. 5).

[31] J. Rustemeyer, A. Melenberg, and A. Sari-Rieger. „Costs incurred by applying computer-aided design/computer-aided manufacturing techniques for the reconstruction of maxillofacial defects“. In: *Journal of Cranio-Maxillofacial Surgery* 42.8 (2014), pp. 2049–2055. URL: `http://dx.doi.org/10.1016/j.jcms.2014.09.014` (cit. on p. 5).

[32] U. Mezger, C. Jendrewski, and M. Bartels. „Navigation in surgery.“ In: *Langenbeck's archives of surgery / Deutsche Gesellschaft f{ü}r Chirurgie* 398.4 (Apr. 2013), pp. 501–514 (cit. on pp. 7, 8).

[33] R. R. Shamir, L. Joskowicz, and Y. Shoshan. „Fiducial optimization for minimal target registration error in image-guided neurosurgery“. In: *IEEE Transactions on Medical Imaging* 31.3 (2012), pp. 725–737 (cit. on p. 7).

[34] L. Franz, M. Isola, D. Bagatto, F. Tuniz, and M. Robiony. „A novel approach to skull-base and orbital osteotomies through virtual planning and navigation“. In: *Laryngoscope* (Aug. 2018) (cit. on p. 8).

[35] A. M. Franz, T. Haidegger, W. Birkfellner, et al. „Electromagnetic tracking in medicine -A review of technology, validation, and applications“. In: *IEEE Transactions on Medical Imaging* 33.8 (2014), pp. 1702–1725 (cit. on p. 8).

[36] G. Eggers. „Image-guided surgical navigation“. In: *Maxillofacial Cone Beam Computed Tomography: Principles, Techniques and Clinical Applications*. Cham: Springer International Publishing, 2018, pp. 1037–1055 (cit. on p. 8).

[37] S. Boutaleb, E. Racine, O. Fillion, et al. „Performance and suitability assessment of a real-time 3D electromagnetic needle tracking system for interstitial brachytherapy“. In: *Journal of Contemporary Brachytherapy* 7.4 (2015), pp. 280–289 (cit. on p. 8).

[38] S. Engelhardt, I. Wolf, S. Al-Maisary, et al. „Intraoperative Quantitative Mitral Valve Analysis Using Optical Tracking Technology“. In: *The Annals of Thoracic Surgery* 101.5 (May 2016), pp. 1950–1956. URL: `https://linkinghub.elsevier.com/retrieve/pii/S0003497516000217` (cit. on p. 8).

[39] R. Seeberger, G. Kane, J. Hoffmann, and G. Eggers. „Accuracy assessment for navigated maxillo-facial surgery using an electromagnetic tracking device“. In: *Journal of Cranio-Maxillofacial Surgery* 40.2 (2012), pp. 156–161 (cit. on pp. 8, 9, 13, 19, 27).

[40] Riitta Seppänen-Kaijansinkko and Risto Kontio. *Contemporary Oral Oncology*. 2017, pp. 341–354 (cit. on p. 9).

[41] N. Komune, K. Matsushima, S. Matsuo, et al. „The accuracy of an electromagnetic navigation system in lateral skull base approaches“. In: *Laryngoscope* 127.2 (2017), pp. 450–459 (cit. on p. 9).

[42] Z. S. Peacock, J. C. Magill, B. J. Tricomi, et al. „Assessment of the OsteoMark-Navigation system for oral and maxillofacial surgery“. In: *Journal of Oral and Maxillofacial Surgery* 73.10 (2015), pp. 2005–2016 (cit. on p. 9).

[43] M. Berger, S. Kallus, I. Nova, et al. „Approach to intraoperative electromagnetic navigation in orthognathic surgery: A phantom skull based trial“. In: *Journal of Cranio-Maxillofacial Surgery* 43.9 (2015), pp. 1731–1736 (cit. on p. 9).

[44] S.-J. Lee, H. J. Yang, M.-H. Choi, et al. „Real-time augmented model guidance for mandibular proximal segment repositioning in orthognathic surgery, using electromagnetic tracking“. In: *Journal of Cranio-Maxillofacial Surgery* (2018) (cit. on pp. 9, 13).

[45] I. Nova, S. Kallus, M. Berger, et al. „Computer assisted positioning of the proximal segment after sagittal split osteotomy of the mandible: Preclinical investigation of a novel electromagnetic navigation system“. In: *Journal of Cranio-Maxillofacial Surgery* 45.5 (2017), pp. 748–754 (cit. on p. 9).

[46] J. M. Bernstein, M. J. Daly, H. Chan, et al. „Accuracy and reproducibility of virtual cutting guides and 3D-navigation for osteotomies of the mandible and maxilla“. In: *PLoS ONE* 12.3 (Mar. 2017). Ed. by J. J. Cray, e0173111 (cit. on pp. 9, 21, 25).

[47] P. Pietruski, M. Majak, E. Swiatek-Najwer, et al. „Accuracy of experimental mandibular osteotomy using the image-guided sagittal saw“. In: *International Journal of Oral and Maxillofacial Surgery* 45.6 (2016), pp. 793–800 (cit. on pp. 9, 21, 22, 27).

[48] J. Nijkamp, K. F. Kuhlmann, O. Ivashchenko, et al. „Prospective study on image-guided navigation surgery for pelvic malignancies“. In: *Journal of Surgical Oncology* 119.4 (2019), pp. 510–517 (cit. on p. 9).

[49] F. Geldof. „Master Thesis Technical Medicine Surgical navigation to guide tumor resections in oncological head and neck surgery“. PhD thesis. University of Twente, 2018 (cit. on pp. 10, 19).

[50] S. Krarup, T. A. Darvann, P. Larsen, J. L. Marsh, and S. Kreiborg. „Three-dimensional analysis of mandibular growth and tooth eruption“. In: *Journal of Anatomy* 207.5 (Nov. 2005), pp. 669–682. URL: `http://doi.wiley.com/10.1111/j.1469-7580.2005.00479.x` (cit. on p. 13).

[51] C. Bettschart, A. Kruse, F. Matthews, et al. „Point-to-point registration with mandibulo-maxillary splint in open and closed jaw position. Evaluation of registration accuracy for computer-aided surgery of the mandible“. In: *Journal of Cranio-Maxillofacial Surgery* 40.7 (2012), pp. 592–598 (cit. on pp. 13, 19, 27).

[52] N. Casap, E. Tarazi, A. Wexler, U. Sonnenfeld, and J. Lustmann. „Intraoperative computerized navigation for flapless implant surgery and immediate loading in the edentulous mandible“. In: *The International journal of oral & maxillofacial implants* 20.1 (2005), pp. 92–98 (cit. on p. 13).

[53] H. T. Luebbers, P. Messmer, J. A. Obwegeser, et al. „Comparison of different registration methods for surgical navigation in cranio-maxillofacial surgery“. In: *Journal of Cranio-Maxillofacial Surgery* 36.2 (2008), pp. 109–116 (cit. on p. 13).

[54] E. Soteriou, J. Grauvogel, R. Laszig, and T. D. Grauvogel. „Prospects and limitations of different registration modalities in electromagnetic ENT navigation“. In: *European Archives of Oto-Rhino-Laryngology* 273.11 (2016), pp. 3979–3986 (cit. on p. 13).

[55] J. B. West, J. M. Fitzpatrick, S. A. Toms, C. R. Maurer, and R. J. Maciunas. „Fiducial Point Placement and the Accuracy of Point-based, Rigid Body Registration“. In: *Neurosurgery* 48.4 (Apr. 2001), pp. 810–817. URL: `https://academic.oup.com/neurosurgery/article/48/4/810/3773362` (cit. on pp. 13, 19).

[56] A. M. R. Cuperus, M. C. Harms, F. A. Rangel, et al. „Dental models made with an intraoral scanner: A validation study“. In: *American Journal of Orthodontics and Dentofacial Orthopedics* 142.3 (Sept. 2012), pp. 308–313. URL: `https://linkinghub.elsevier.com/retrieve/pii/S0889540612004908` (cit. on p. 20).

[57] P. Pietruski, M. Majak, E. Swiatek-Najwer, et al. „Image-guided bone resection as a prospective alternative to cutting templates - A preliminary study“. In: *Journal of Cranio-Maxillofacial Surgery* 43.7 (2015), pp. 1021–1027 (cit. on p. 21).

[58] A. Fedorov, R. Beichel, J. Kalpathy-Cramer, et al. „3D Slicer as an image computing platform for the Quantitative Imaging Network“. In: *Magnetic Resonance Imaging* 30.9 (2012), pp. 1323–1341 (cit. on p. 22).

[59] S. G. Brouwer de Koning, T. P. ter Braak, F. Geldof, et al. „Resection planes in mandibular surgery: preoperative planning, intraoperative placement and postoperative evaluation. Unpublished manuscript.“ In: (2019) (cit. on p. 25).

[60] A. Wagner, K. Schicho, W. Birkfellner, et al. „Quantitative analysis of factors affecting intraoperative precision and stability of optoelectronic and electromagnetic tracking systems“. In: *Medical Physics* 29.5 (2002), pp. 905–912 (cit. on p. 27).

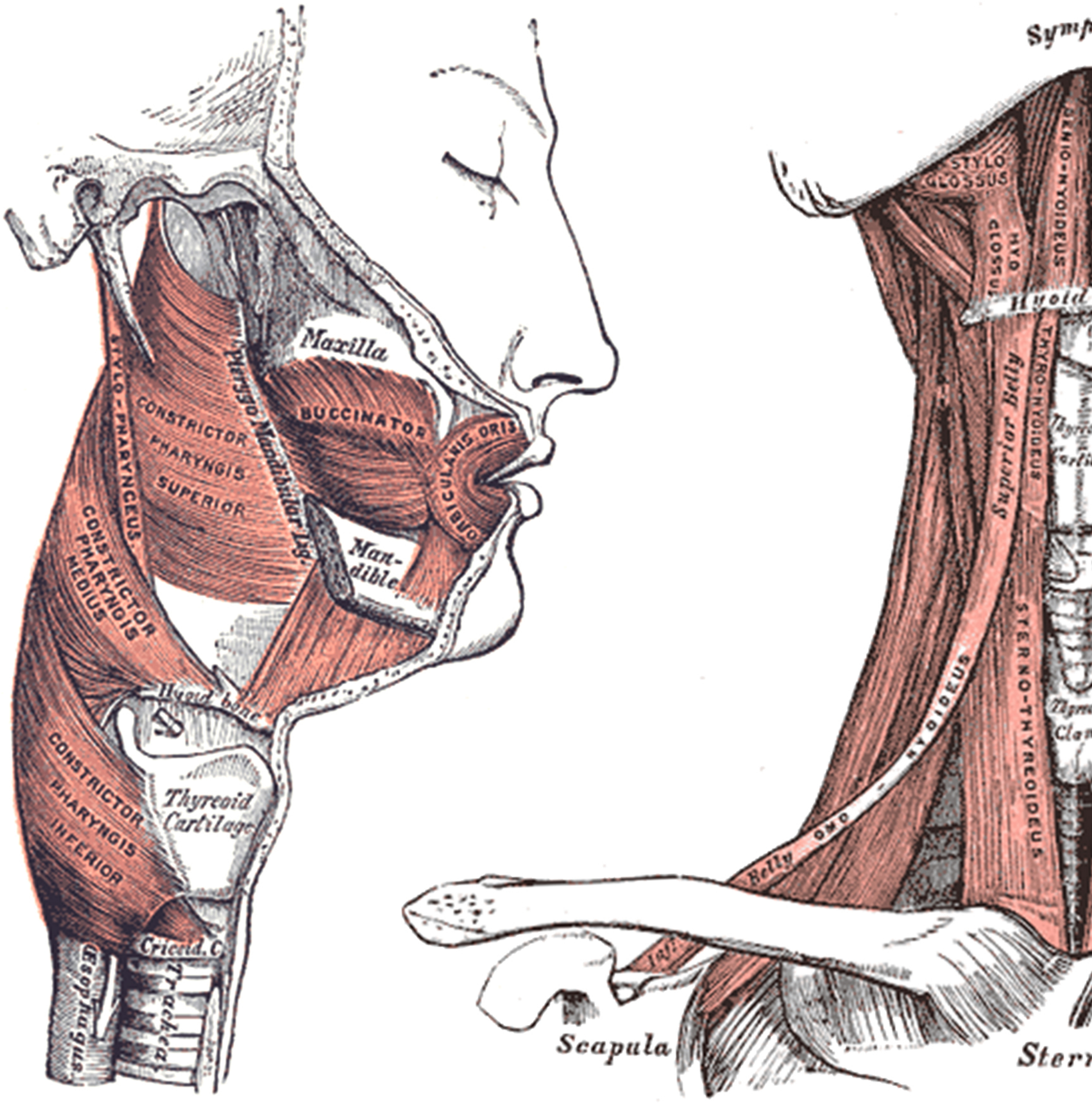
Maxilla
BUCCINATOR
ORBICULARIS ORIS
Pterygo Mandibular Lig.
CONSTRICTOR
PHARYNGIS
SUPERIOR
STYLO-PHARYNGEUS
CONSTRICTOR
PHARYNGIS
MEDIUS
Man-
dible
Hyoid bone
Thyroid
Cartilage
CONSTRICTOR
PHARYNGIS
INFERIOR
Cricoid C.
Trachea
Œsophagus
STYLO
GLOSSUS
HYO
GLOSSUS
GENIO-HYOIDEUS
Hyoid
THYRO-HYOIDEUS
Superior Belly
STERNO-THYREOIDEUS
OMO-HYOIDEUS
Belly
Scapula